

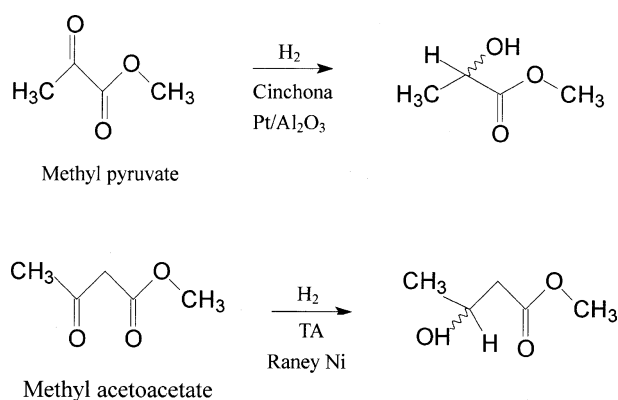
Surface structure of heterogeneous catalysts: Cinchona and tartaric acid on solid surface

Dong Wang, Hui-Juan Yan, Qing-Min Xu, Mei-Juan Han, and Li-Jun Wan*

Institute of Chemistry, Chinese Academy of Sciences, Beijing, 100080, China

Enantioselective hydrogenation by heterogeneous catalysts has gained great importance in organic synthesis, chemical engineering and pharmaceutical industry. However, the mechanism of enantioselectivity is not well understood due to the absence of evidence at the molecular level. Recently, the great advance on this topic has been made by applying scanning tunneling microscopy (STM) and other surface characterization techniques to get direct evidence about the enantioselective mechanism of catalysts. Here, the progress on the adsorption mode of chiral modifiers such as cinchona and tartaric acid and the related enantioselective mechanism is reviewed from the viewpoint of surface science. Particularly, some STM works on this topic are summarized. Finally, several key issues for further investigation are outlined.

The synthesis of optically pure chiral compounds has gained great importance in organic chemistry, pharmaceutical chemistry, and catalytic chemistry. At present, the effective way to synthesize enantiopure chemicals is *via* homogeneous catalysis. However, much attention has been paid towards obtaining chiral products by heterogeneous catalysis because of the special advantage of heterogeneous catalysts in handling, separation, stability, and recovery [1–8]. One possible candidate for heterogeneous asymmetry catalysts is the natural chiral metal surfaces in view of the enantioselectivity adsorption of chiral chemicals on them [9–11]. However, the natural chiral surface with high miller index is always difficult to obtain and hard to handle, which limits its application in catalysis. Another strategy promising and demonstrated to be successful to obtain chiral catalysts is *via* chiral modification of the achiral catalytically active site with chiral auxiliary (modifier) [12–15]. Two such catalytic systems for enantioselective hydrogenation reactions are Pt/Al₂O₃ catalysts in the presence of different cinchona alkaloids and tartaric acid (TA) modified Ni catalysts [1–8,14,15]. These catalysts have been shown to be effective for performing enantioselective hydrogenation on a wide range of C=O bond-containing molecules with high enantiomeric excess of up to 90–95% [1]. Scheme 1 shows the typical catalytic reaction associated with the two catalysis systems. As can be seen, the substrates associated with the Cinchona/Pt catalysts and TA/Ni are α and β -ketoester, respectively.



Scheme 1. Schematic representation of asymmetric hydrogenation of α - and β -ketoester on cinchona modified Pt/Al₂O₃ and TA modified Raney Ni catalysts, respectively.

To obtain catalysts with high activity and enantioselectivity, considerable effort has been undertaken to screen out the high effective modifier molecules and optimize reaction conditions such as solvents, temperature, modifier concentration, and catalyst supports. At the same time, the investigation on the catalysis mechanism, including the adsorption mode of modifiers on catalysts, the structure of active intermediates, and dynamics of their transformation to products, was also intensively carried out. Various surface and interface characterization techniques have been applied to investigate the enantioselective mechanism of these two catalysis systems. Among them, the application of scanning tunneling microscopy (STM) to this topic is of particular interest because of its sub-molecular resolution and real-space observation ability [12,13].

*To whom correspondence should be addressed.
E-mail: Wanlijun@iccas.ac.cn

Because the study on the mechanism of enantioselective catalysis is still in their starting point, there are many unclear issues in this topic. The investigations on surface ordering, adlayer symmetry and molecular orientation are of wide interests. From the previous TA on Cu(110) [12], progress has been made about the adsorption mode of modifiers on the catalysts and the interaction between the modifiers and reactants. Several enantioselective mechanisms have been proposed on the basis of the obtained results. In this article, the state-of-the-art of mechanism investigation of the heterogeneous asymmetry catalysis with cinchona and tartaric acid is reviewed from the viewpoint of surface science. Particularly, interesting STM works on this topic are summarized. Finally, some important projects need further efforts are outlined.

1. Cinchona/Pt catalyst and cinchona adsorption on Cu(111)

To get the insight into the heterogeneous catalysis process, it is necessary to know the exact adsorption mode of modifiers and interaction between the modifiers and reactants on the catalyst surface. It is believed that the conformation of cinchona modifier on Pt surface is closely related to the efficiency and enantioselectivity of the catalysts [16–19]. The development of surface science provides the new viewpoint to investigate the adsorption of modifiers on catalyst surface. So far, various modern surface analysis techniques and theoretical simulations have been applied to study the adsorption mode of cinchona, particularly cinchonidine (Cd) and cinchonine (Cn), on surface under simulated or real catalysis environment. For example, near-edge X-ray adsorption fine structure (NEXAFS) investigation revealed that 10,11-dihydrocinchonidine (HCd) molecules take parallel orientation by quinoline ring at 25 °C and tilted orientation at 50 °C on Pt(111) surface under high vacuum (UHV) condition [16]. Carley *et al.* [17] found that HCd molecules form disordered stable monolayer on Pt(111) in UHV conditions by X-ray photoelectron spectroscopy (XPS) and low-energy electronic diffraction (LEED). Biirgi and Baiker [18] demonstrated that Cd molecules have three stable conformations in solution and the population of the conformers depends on the dielectric constant of solvents by combining DFT calculation and NMR. Recently, other *in situ* methods such as reflection – adsorption infrared spectroscopy (RAIRS), attenuated total reflection IR spectroscopy (ATR-IRS), and surface-enhanced Raman spectroscopy (SERS) were also employed to study the adsorption of Cd in solution [19–23]. Parallel orientation *via* the quinoline ring was observed, while at higher concentration Cd with tilted orientation was also observed. The effect of solvent and coverage on the adsorption mode was discussed.

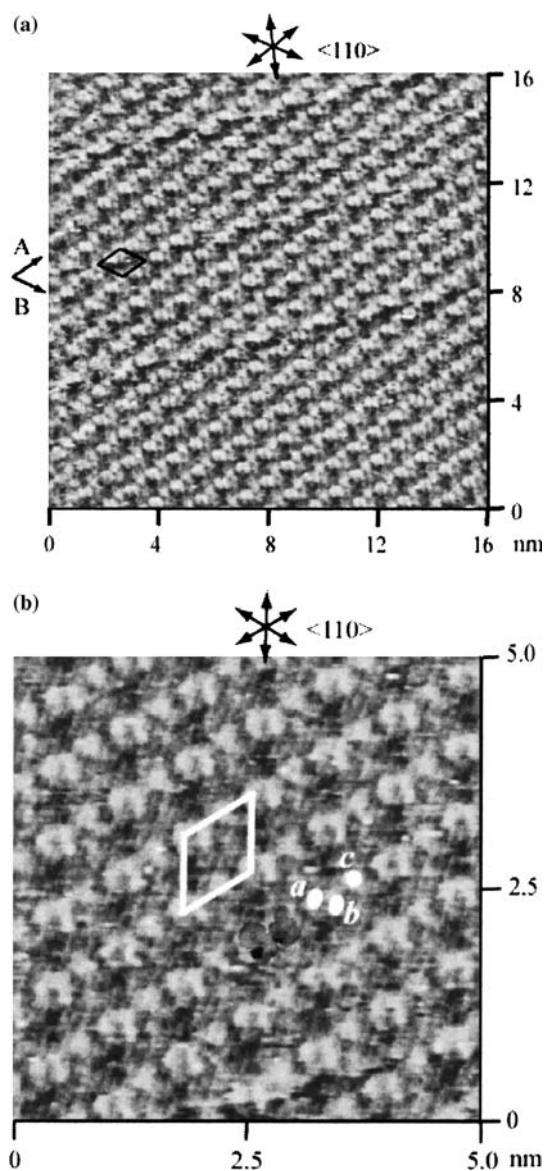


Figure 1. (a) STM image of Cd adlayer on Cu(111) in 0.1 M HClO_4 + 0.1 mM Cd at -0.287 V with a setpoint of 10 nA. (b) High resolution STM image of Cd molecules on Cu(111) with a setpoint of 10 nA.

STM is a powerful tool for the investigation of adsorption mode of molecules on surface. The direct chiral discrimination of chiral molecules at solid/liquid interface and the successful investigation of chiral adlayer orderliness of enantiomers and racemic mixtures by using ECSTM working in solution encourage us to investigate the adsorption mode of chiral modifiers on solid surface such as Cu as the preliminary study [24,25]. With the high resolution of ECSTM, the adsorption of two widely used cinchona alkaloids modifier: Cd and Cn was studied. As a preliminary study of cinchona with STM, the direct evidence on adsorption mode of cinchona modifier on Cu(111) surface was obtained [26,27].

Figure 1(a) shows a typical STM usage of Cd adlayer on 0.1 M HClO₄ + 0.1 mM Cd. It can be seen that the directions of molecular rows indicated by A and B are along close-packed directions of Cu(111) lattice with a period of 1.01 ± 0.02 nm corresponding to four times of the Cu(111) lattice. The angle between A and B is $60 \pm 2^\circ$. Therefore, a (4×4) structure of the molecular adlayer can be concluded. A unit cell is outlined in figure 1(a). In contrast, no ordered structure of Cd on Pt(111) was reported by LEED in UHV [17]. Figure 1(b) shows a higher resolution STM images to reveal the internal structure of Cd molecules. It can be clearly seen that each Cd molecule consists of spots *a*, *b* in ellipse shape and *c* in round shape. The distance between spots *a* and *b* is measured to be 0.48 ± 0.02 nm, while that between *a* and *c* is measured to be 0.83 ± 0.02 nm.

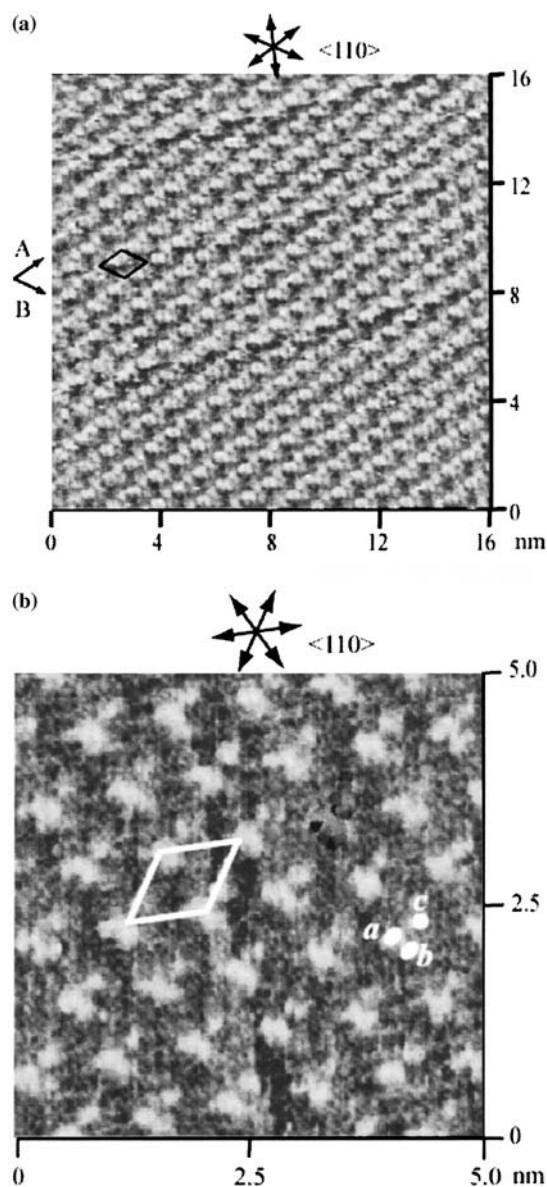


Figure 2. (a) STM image of Cn adlayer on Cu(111) in 0.1 M HClO₄ + 0.1 mM Cn at -0.287 V with a setpoint of 10 n A. (b) High resolution STM image of Cn molecules on Cu(111) with a setpoint of 10 nA.

With the similar procedure, the Cn adlayer was prepared on Cu(111) in 0.1 M HClO₄. Although Cd and Cn are diastereomeric pairs, they are always called “pseudo- or near-enantiomers” because their opposite stereochemistry at the crucial carbons C8 and C9. In fact, the Pt catalysts modified with Cd or Cn can catalyze the same prochiral reactant to generate nearly identical values of enantiomeric excess but with a reversal of the sign. Similar to that of Cd, a well-defined adlayer is obtained as shown in figure 2(a). The molecular rows are seen to extend along the $\langle 110 \rangle$ directions of Cu(111) substrate as indicated by the arrows in figure 2(a). The intermolecular distance along the molecular rows is *ca.* 1.00 nm, nearly four times of the lattice distance of Cu(111). Thus, Cn, similar to Cd, form a (4×4) adlayer structure on Cu(111). The results indicate that the adlayer symmetry is not affected by the chirality of molecules. Figure 2(b) shows a high resolution STM image of the Cn adlayer on Cu(111) in 0.1 M HClO₄ obtained at -0.287 V. Each Cn molecule consists of three bright spots labeled by *a*, *b*, and *c*. The distance between *a* and *b* is measured to be 0.49 ± 0.02 nm and 0.85 ± 0.02 nm between *a* and *c*. The corrugation height of *a* and *c* is disclosed from the cross-section profile.

The STM images obtained at both Cd and Cn adlayers are found to be very stable. To investigate the potential-dependent adsorption behavior of molecules, the electrode potential was scanned in the double layer potential range during the experiment. The STM image is consistently obtained in the potential range of -0.3 – 0.0 V. No potential dependent orientation change and redox chemistry of molecules was found in the experiment. This result is in accordance with the cyclic voltammetry measurement. In fact, the featureless cyclic voltammograms (CVs) was obtained after the addition of Cd or Cn in the cyclic voltammetry measurement, indicating no electrochemical reaction involving in the double layer potential region, although the electric charge involved in the double layer becomes smaller due to the molecular adsorption. Similar CVs were obtained on Cd and Cn modified Cu(111) electrode because the single crystal surface in low miller index with high symmetry has no enantioselectivity towards chiral molecules. Attard reported an electrochemical study on the adsorption of Cd on achiral and chiral single crystal Pt surface [9]. Two pairs of redox process were identified independent of the chirality of surface, indicating no selectivity of the adsorption of Cd on Pt surface. Detailed investigation suggests the peaks correspond to the adsorbate-blocked H₂ adsorption/desorption. Similar result was reported on the adsorption of Cd on polycrystalline Pt electrode [28].

Cinchona is composed of quinuclidine moiety and planar quinoline moiety interconnected by two carbon-carbon single bonds. The difference between Cd and Cn and other cinchona derivatives is the chirality of

interconnecters C8 and C9. The detailed investigation of the dependence of the enantioselectivity of cinchona alkaloid based catalysts on the structures of the derivatives and the spectra results indicate that the quinoline group is the anchoring group for the cinchona modifier, while the quinuclidine moiety is responsible for the enantioselectivity [14–23]. Meanwhile, A flat-on conformation of the pyridine and naphthalene, the molecules with similar structural features to quinoline moiety, on Cu(111) was proposed on the basis of *in Situ* STM observation [29,30]. On the basis of above results, it is proposed that spots *a* and *b* correspond to two aromatic ring of the quinoline moiety with a flat-on orientation on Cu(111) surface. After Comparing the STM image with chemical structure of Cd, the spot *c* is believed to be produced by the quinuclidine moiety. Because of the special steric structure of Cd, the quinuclidine moiety should extend out of the surface. A possible structural model for Cd molecules on Cu(111) is tentatively proposed in figure 3(a). The

nitrogen atom in quinoline moiety is located on atop sites [30]. The rings of quinoline are slightly shifted from the twofold bridge sites of Cu(111) lattice, similar to the adsorption geometry of naphthalene [29]. The line connected the quinoline and quinuclidine is aligned along the close-packed direction of the underlying Cu(111) lattice as STM images revealed. In the model, quinoline rings take parallel orientation to Cu(111) surface. Similarly, the structure model for Cn adlayer on Cu(111) was proposed in figure 3(b). The mirror symmetry between two adsorption structures can be found because of the pseudo-enantiomeric relationship between two molecules.

Aside from the adsorption mode of modifiers on catalysts, another important problem associated with the catalytic process is the interaction between the modifiers and reactants. Lambert and co-workers [31] investigated the interaction of (S)-(-)-1-(1-naphthyl)ethylamine (NEA) modifier with methyl pyruvate (MP) reactant in UHV. A disordered adlayer of (S)-NEA on Pt(111) was found by STM observation. At 300 K, both in the presence and absence of coadsorbed hydrogen, disordered adlayer of (S)-NEA was observed. The thermodynamic evolution of adlayer was investigated at elevated temperature and the possible origin of enantioselectivity destroy at high temperature was indicated. Then, MP molecules were introduced to the system to study the interaction between the reactant and modifier molecules. The dimer structure differing from both the (S)-NEA and MP adlayers was found in the STM images. Detailed analysis indicated the dimers correspond to 1:1 docking complexes between the prochiral reactants and the chiral modifiers. The result provides a direct evidence for the 1:1 interaction mechanism between modifiers and reactants in cinchona/Pt based catalysts. The enantioselectivity of product is determined by the chirality of modifier. The same group also carried out the intensive investigation of the adsorption and reactivity of MP on Pt(111) by STM, NEXAFS, and XPS in the absence and the presence of coadsorbed hydrogen. The result provides some important hints for the irreversible deactivation of catalysts during start-up or steady-state operation of Pt catalysts [32,33].

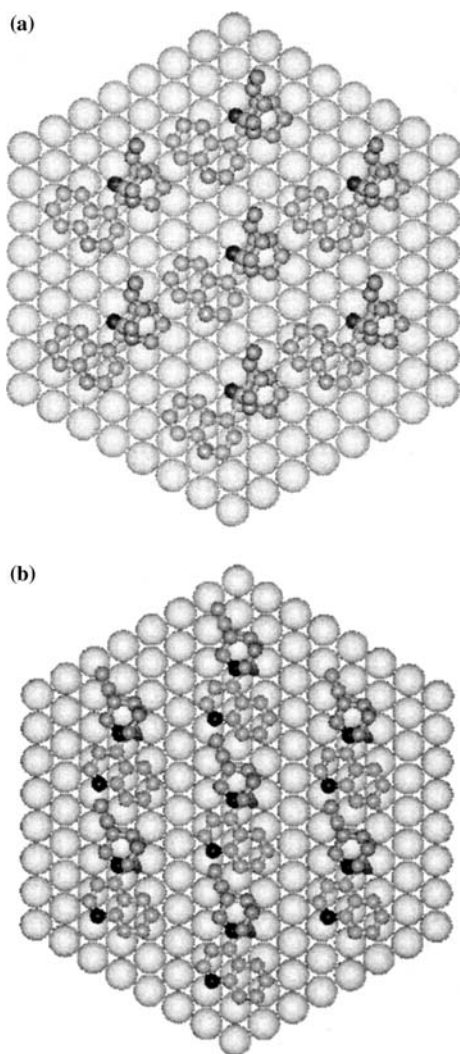


Figure 3. Structural models proposed for Cd (a) and Cn (b) adlayer on Cu(111).

2. TA adsorption on Cu and Ni

TA modified Raney Ni (Ni:Al = 42:58) nanoparticle is high-efficient catalysts for the hydrogenation of β -ketoester with high enantioselectivity. The modification of Ni catalysts by TA is always achieved in aqueous media, or sometime alcohol solution. The detailed investigation of the effect of modification solvents, the modification time and temperature, modifier concentration, and the incorporation of NaBr as a comodifier on the uptake of TA and on the ultimate activity and

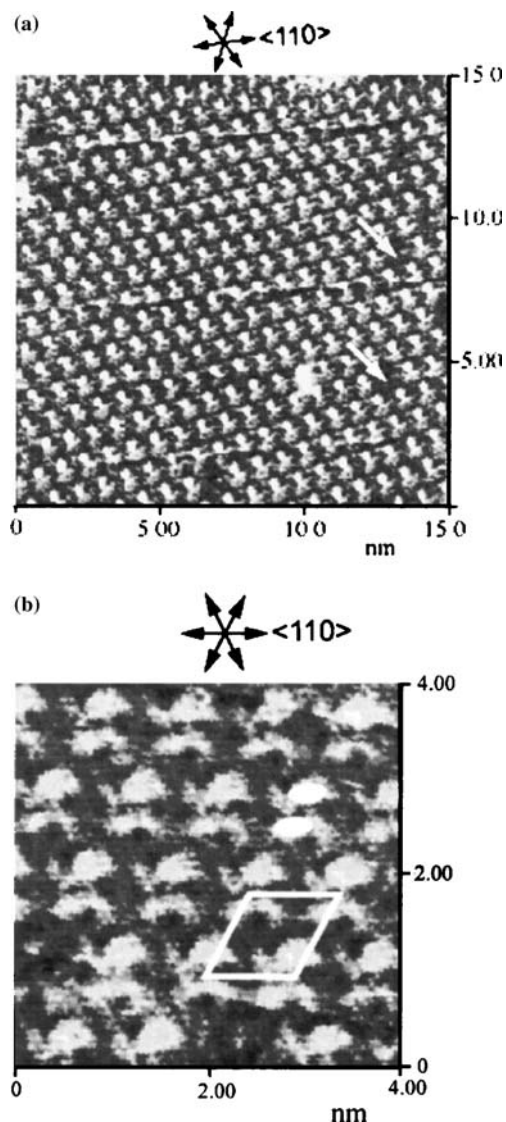


Figure 4. (a) STM top view of R,R-TA adlayer at -0.20 V with a setpoint of 10 nA. Scanning rate was 10 Hz. (b) High-resolution STM image of the R,R-TA adlayer at -0.20 V.

enantioselectivity was carried out [34–36]. Several possible mechanisms for the enantioselectivity have been proposed [37,38].

ECSTM investigation was performed to study the adsorption structure of TA on Cu(111) surface in aqueous solution [39]. Figure 4(a) is a typical large scale STM image of R,R-TA adlayer acquired at -0.20 V. A well-ordered adlayer of molecules was observed on the wide atomically flat terrace. TA molecules appear as ordered bright spots with some defects as indicated by arrows in figure 4(a). The molecular rows cross each other at an angle of either 60 or 120° within an experimental error of $\pm 2^\circ$. It is found that all molecular rows are almost perfectly parallel to the underlying Cu(111) atomic rows. The distance between neighboring bright spots along the close-packed direction of Cu(111) is measured to be $ca. 0.98 \pm 0.02$ nm, about four times

the lattice parameter of Cu(111). On the basis of the intermolecular distance and orientation of molecular rows, a (4×4) structure for the adlayer can be concluded. A unit cell is superimposed in the higher resolution image of figure 4(b) showing more details of the internal structure and coordination of each TA molecule. It is clearly seen in the image that each bright spot appears in a pair of lobed spots as outlined by two ellipses in figure 4(b). The length of a pair of lobed bright spot is $ca. 0.6$ nm close to the size of TA molecules (0.5 nm) [40]. It could be assumed that each bright spot may arise from a molecule. Two individual lobed spots in a pair are separated by $ca. 0.4$ nm. The distance admits the formation of intermolecular H-bonds between the acid groups and OH groups in the pair molecules. The structural details will be discussed in next part.

S,S-TA adlayer was also prepared on Cu(111). A well-defined adlayer similar to R,R-TA is observed in large scale STM images. A high resolution STM image is shown in figure (5). It is surprising that the features of S,S-TA molecules in figure 5 are very similar to those of R,R-TA in figure 4(b). S,S-TA molecules show two-lobed bright spots indicated by two ellipses in figure 5. It is temporarily proposed that each bright spot may arise from a molecule. Two individual lobed spots form a molecular pair separated by $ca. 0.4$ nm. The same (4×4) structure was determined by analyzing the symmetry of the adlayer to the Cu(111) substrate. The results described above demonstrate that both R,R-TA and S,S-TA molecules form ordered structures on Cu(111) in aqueous solution.

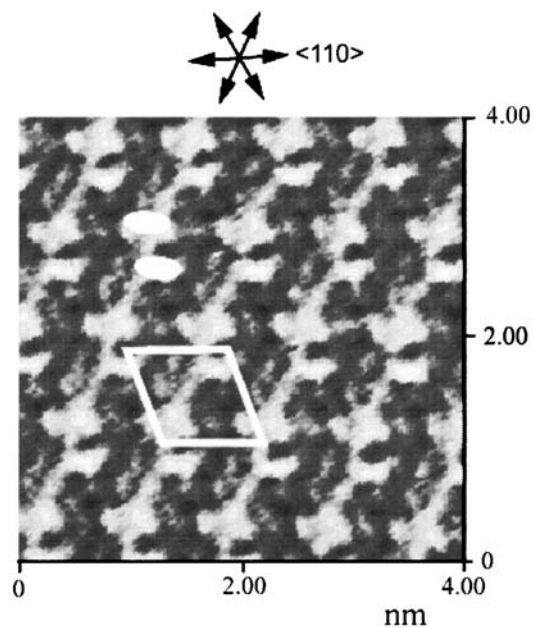


Figure 5. High-resolution STM image of the S,S-TA adlayer at -0.20 V with a setpoint of 10 nA. Scanning rate was 13 Hz.

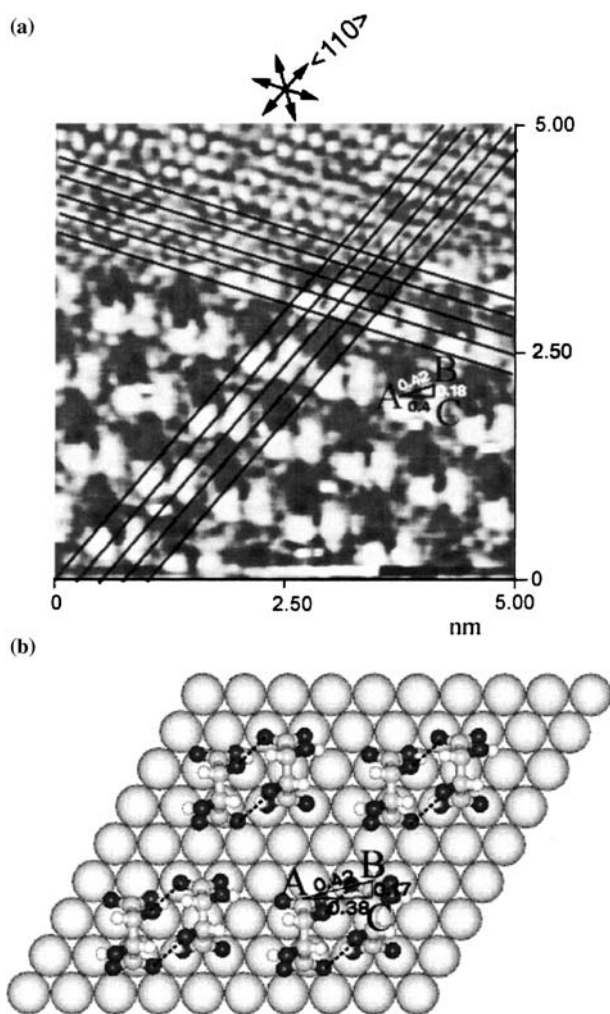


Figure 6. (a) Composite STM image in 0.1 M HClO_4 + 1 mM R,R-TA. The upper part shows the atomic structure of Cu(111) substrate and the lower part R,R-TA adlayer. Scanning rate was 15 Hz. Setpoint was 3 nA. (b) The proposed model for R,R-TA adlayer on Cu(111).

To further understand the adsorption of TA molecule on Cu(111) substrate such as adsorption site and symmetry, a composite STM imaging was performed by stepping potentials in the solution containing R,R-TA molecules, as shown in figure 6(a). The lower part of the frame was imaged at -0.20 V and upper part was imaged at -0.39 V, when imaging direction from bottom to top. The upper part of the STM image clearly shows the (1×1) atomic structure of Cu(111) substrate. The lower part shows the two-lobed bright spots of R,R-TA molecule. A geometric network is imposed on the image based on the Cu(111) lattice. The (4×4) symmetry for the adlayer is further demonstrated by the extended lines in the network along the close-packed atomic rows of the underlying Cu(111) substrate.

From the composite STM image, we try to propose a structural model for the adsorption of R,R-TA mole-

cules on Cu(111). It is clear that if the two bright spots in a pair was treated as a single R,R-TA molecule, there is more space in the (4×4) structure. Therefore, we propose that the two bright spots in a pair are two individual R,R-TA molecules, which form a dimeric structure. A careful observation found that the two bright spots in STM image of figure 6(a) show different contrast, which implies that two molecules in a dimer may adsorb on different adsorption sites of Cu(111). The intermolecular distances of two bright spots can be illustrated in figure 6(a) with *ca.* 0.40 nm in AC direction; *ca.* 0.42 nm in AB direction and *ca.* 0.18 nm in BC direction.

Each TA molecule includes four carbon atoms. The chirality of TA molecules arises from the different orientation of two hydroxyl groups on C2 and C3. Two carboxyl groups are at the ends of molecule (C1 and C4), respectively. According to the results of IR spectroscopic studies, carboxylic acids, such as formic [41,42], benzoic [43,44] and citric acid [45,46], adsorb on noble metal surface with the carboxylate form. Previous results have shown that the oxygen atoms of the carboxylate groups favorably adsorb on the top sites in a short bridge [47–51]. Furthermore, a bend geometry for the adsorption of R,R-TA molecules on Cu(110) surface has been proposed [12,40,51,52]. Hence, on the basis of the above-mentioned results and the obtained STM data, one possibility for the adsorption of R,R-TA is assumed that each TA molecule coordinates with Cu surface deprotonates fully and locates on the top sites of Cu(111) substrate with a bend geometry. In this configuration, two molecules in a dimer should show the identical appearance in STM images. However, different contrast between the two bright spots indicate different adsorption model between the two molecules. If the oxygen atoms in carboxyl groups in the dimer adsorb on the different sites of Cu atoms, the STM image will show contrast difference. Therefore, we propose a structural model in figure 6(b). In this model the oxygen atoms of carboxyl end groups in the left R,R-TA molecule are located on the bridge sites and the right R,R-TA molecule on the top sites of Cu(111) lattice. The tartaric acid is in a bicarboxylate form. The intermolecular distances in the model are almost consistent with the measured distances in STM images. On the other hand, two R,R-TA molecules in a dimer can form H-bonds between the OH groups and carboxyl groups, as shown in figure 6(b) in dashed lines. Each R,R-TA molecule can leave a hydroxyl group protruding into solution to form H-bonds with other reactant species. A similar adsorption model for S,S-TA molecules is also proposed (not shown here).

Note that there are three forms in existence for tartaric acid according to the study in UHV: bicarboxylate, monocarboxylate or biacid [40]. Although the TA molecules in the model of figure 6(b) are the form of

bicarboxylate, the real form of TA species on Cu(111) surface cannot be totally determined by only STM. More techniques such as IR and theoretical calculation are necessary.

In a relatively earlier work, Lozenzo *et al.* [12,40,52] investigated the adsorption and assembly of TA on Cu(110) in UHV. Several different adsorption structures depending on the coverage and temperature were observed by STM and confirmed by LEED, and the detailed information of the adsorption orientation and registry of TA on the surface was deduced from the RAIRS results. One of the most interesting results obtained from the work is the so-called chiral surface formed by a special adsorption phase. In this phase, the TAs existing as bitartrate are assembled in groups of three and leave empty chiral channels on Cu(110) surface. The chiral channel in the adlayer provides a chiral environment to accommodate the achiral reactants. The result provides an experimental evidence for the template mechanism for the enantioselectivity of the heterogeneous catalysts. The special symmetry of substrate, adsorbates, and the adlayer resulted in the absence of the rotation and mirror domains. Thus, the whole surface was covered with this chiral phase and the entire chiral surface was created. Barbosa and Sautet [51] conducted the theoretical simulation and proposed the adsorption of bitartrate on Cu(110) results in the relaxation of Cu atoms, which accounts for the formation of chiral channels.

Then, the same group transfer their interests to the adsorption of TA on Ni(110), a system closer to the real catalyst [13]. Surprisingly, the disordered adlayer, entirely different from that on Cu(111), was observed. A DFT theoretical simulation indicates the surface Ni atoms undergo relaxation or reconstruction upon molecular adsorption. They proposed that the chiral character of modifier was bestowed on the reconstructed surface and resulted in the enantioselectivity of the catalysts.

Very recently, Jones and Baddeley [53] conducted the similar STM investigation of the adsorption of TA on Ni surface in UHV. In the experiment, Ni(111) surface was chosen because it is the most thermodynamic stable surface, especially for the real catalysts, in which Ni nanoparticle with size of 3–5 nm is dominant. Contrary to the adlayer structure of TA on Ni(110), three ordered adlayer depending on the temperature were observed. It is believed that the ordered TA adlayers can provide ordered array of vacancies on metal surface available for β -ketoester molecules to adsorb. Because of the chirality of TA molecules surrounding the vacancies, ketoester molecules only can dock onto vacancies at one direction in order to form H-bonding with OH groups of neighboring TA molecules. If all ketoester species are adsorbed on vacancies with the same face attached to the surface, the dominant product by the hydrogenation of reactant

molecules will be one of the two possible enantiomers. The enantioselectivity is created. However, it is possible that some relaxations of the surrounding TA molecules may occur according to the size of reactant molecules. In fact, when MAA was introduced to the R,R-TA modified Ni(111), MAA can locally rearrange the TA adlayer to produce a two-dimensional co-crystal [54]. Nevertheless, the adsorption geometry of ketoesters molecules will be defined by H-bonding between the reactants and TA.

3. Discussion

For the heterogeneous catalysts, three important factors: the adsorption sites, the adsorption conformation of modifiers on surface, and the adlayer structure are all of special importance for the catalysis process and the enantioselectivity. By the combination of various surface analytic techniques, detailed insight into the adsorption mode of modifier on catalysts surface has been obtained. For example, the adsorption of Cd(Cn) on surface by quinoline moiety has been deduced from STM results and in accordance with the other results obtained previously [26,27]. Because of the special steric structure of Cd(Cn), the quinuclidine moiety should extend out of the surface, which facilitate the interaction of cinchona modifiers with the reactants. The adsorption structure of TA on Cu(110), Cu(111), Ni(110), Ni(111) surface has been extensively studied by applying STM and other surface characterization methods [12,13,39,40,51–54]. Although several different adlayer structures have been found, it is generally accepted that the TA molecules anchor on the surface with deprotonated carboxyl groups. Thus, the H-bonding interaction between the freely-stretched OH groups and the C=O in reactants will define the special conformation of reactants on surface. The second contribution from the STM results is the important role of the adlayer structure played in the enantioselective catalysis. There are three mechanisms proposed for the enantioselective heterogeneous catalysis. First, the modifier molecules anchored on the catalysts interact with the upcoming reactants to form 1:1 complexes [31]. The conformation of reactants was defined by the modifier-reactant interaction and the chirality of modifiers, which is responsible for the enantioselectivity. Note that in this mechanism, the chiral environment surrounding the reactants only comes from one modifier. In the second mechanism named “template mechanism”, the two-dimension chiral adlayer was formed after the modifier adsorption. The typical examples include the chiral channels on Cu(110) upon adsorption of TA and chiral screws created by the adsorption of dithiol-binaphthalene on Au(111) [12,55]. The adsorption conformation of the prochiral reactants will be determined by the chiral template. The role of TA in the two-dimensional co-crystal of TA and MAA

on Ni(111) can be thought as a slightly modified template [54]. The adlayer structure of TA on Cu(111) in aqueous solution also favors the template mechanism [39]. In addition, the template mechanism opens a new routine for catalysts design with the high enantioselectivity in view of the relative ease to construct two-dimensional chiral adlayers on surface. For example, the chiral “screws” created on Au (111) upon adsorption of dithiol-binaphthalene show enantioselectivity towards amino acids adsorption [56]. Finally, some researchers proposed that some chiral kinks on catalysts nanoparticle, both formed naturally or induced by the chiral modifier adsorption, are the adsorption centers for prochiral reactants and responsible for the enantioselectivity. The representative examples include the chiral reconstruction of Ni(110) induced by TA adsorption and the chiral faceting of Cu(100) upon L-lysine adsorption [13,57]. Recently, Attard *et al.* [58] proposes the enantioselectivity of cinchona/Pt catalysts is related to the chiral kinks at the corner of catalysts nanoparticles by the combination of electrochemistry and STM observation.

Finally, we should point out that the results presented here are only a preliminary step toward the full understanding of the catalytic mechanism of heterogeneous enantioselective catalysts. We should be highly cautious to apply the obtained result to explain the real catalysis process because most of experimental results were obtained in the model systems, such as in UHV, on ideal single-crystal surface. Thus, the most urgent requirement is to carry out *in situ* investigation on the adsorption of modifiers on catalysts surface to get the insight into the real catalysis process. The modifiers always have different adsorption behavior on different metal surface. The robust example may be the entirely different adlayer structure of tartaric acid on Cu(110) and Ni(110) [12,13]. In addition, the effect of the environment, for example, UHV vs solvent, including the polarity of the solvent, should also be paid great attention. Finally, the investigation of the interaction between the modifiers and reactants is obviously important, although it is very difficult to study and requires the combination of different analysis techniques.

References

- [1] A. Baiker, *J. Mol. Catal. A: Chem.* 115 (1997) 473.
- [2] H.-U. Blaser, *Tetrahedron: Asymmetry* 2 (1991) 843.
- [3] A. Baiker, *J. Mol. Catal. A: Chem.* 163 (2000) 205.
- [4] M. Studer, H.-U. Blaser and C. Exner, *Adv. synth. Catal.* 345 (2003) 45.
- [5] T. Osawa, T. Harada and O. Takayasu, *Top. Catal.* 13 (2000) 155.
- [6] H.-U. Blaser, H.P. Jalett, M. Müller, and M. Studer, *Catal. Today* 37 (1997) 441.
- [7] M. Von Arx, T. Mallat and A. Baiker, *Top. Catal.* 19 (2002) 75.
- [8] A. Pfaltz and T. Heinz, *Top. Catal.* 4 (1997) 229.
- [9] G.A. Attard, *J. Phys. Chem. B* 105 (2001) 3158.
- [10] D.S. Sholl, A. Asthagiri and T.D. Power, *J. Phys. Chem. B* 105 (2001) 4771.
- [11] J.D. Horvath and A.J. Gellman, *J. Am. Chem. Soc.* 124 (2002) 2384.
- [12] M.O. Lorenzo, C.J. Baddeley and C. Muryn, R. Raval, *Nature* 404 (2000) 376.
- [13] V. Humblot, S. Haq, C. Muryn, W.A. Hofer and R. Raval, *J. Am. Chem. Soc.* 124 (2002) 503.
- [14] H.-U. Blaser, H.P. Jalett, W. Lottenbach and M. Studer, *J. Am. Chem. Soc.* 122 (2000) 12675.
- [15] K. Kacprzak and J. Gawroński, *Synthesis-Stuttgart* (2001) 961.
- [16] T. Evans, A.P. Woodhead, A. Gutiérrez-Sosa, G. Thornton, T.J. Hall, A.A. Davis, N.A. Young, P.B. Wells, R.J. Oldman, O. Plashkevych, O. Vahtras and H. Ågren, V. Carravetta, *Surf. Sci.* 436, (1999) L691.
- [17] A.F. Carley, M.K. Rajumon, M.W. Roberts and P.B. Wells, *J. Chem. Soc. Faraday Trans.* 91 (1995) 2167.
- [18] T. Bürgi, and A. Baiker, *J. Am. Chem. Soc.* 120 (1998) 12920.
- [19] D. Ferri, T. Bürgi, and A. Baiker, *Chem. Commun.* (2001) 1172.
- [20] D. Ferri, and T. Bürgi, *J. Am. Chem. Soc.* 123 (2001) 12 074.
- [21] J. Kubota, and F. Zaera, *J. Am. Chem. Soc.* 123 (2001) 11 115.
- [22] J. Kubota, Z. Ma and F. Zaera, *Langmuir* 19 (2003) 3371.
- [23] W. Chu, R.J. LeBlanc and C.T. Williams, *Catal Commun.* 3 (2002) 547.
- [24] Q.-M. Xu, D. Wang, L.-J. Wan, C. Wang, C.-L. Bai, G.-Q. Feng and M.-X. Wang, *Angew. Chem. Int. Ed.* 41 (2002) 3408.
- [25] D. Wang, Q.-M. Xu, L.-J. Wan, C.-L. Bai and G. Jin, *Langmuir* 19 (2003) 1958.
- [26] Q.-M. Xu, D. Wang, L.-J. Wan, C.-L. Bai, Y. Wang, *J. Am. Chem. Soc.* 124 (2002) 14 300.
- [27] Q.-M. Xu, D. Wang, M.J. Han, L.-J. Wan and C.-L. Bai, *Langmuir* 20 (2004) 3006.
- [28] I. Bakos, S. Szabó, M. Bartók, E. Kálmán, *J. Electroanal. Chem.* 532 (2002) 113.
- [29] L.-J. Wan, K. Itaya, *Langmuir* 13(1997) 7173.
- [30] D. Wang, Q.-M. Xu, L.-J. Wan, C.-L. Bai, *Langmuir* 18 (2002) 5133.
- [31] J.M. Bonello, F.J. Williams and R.M. Lambert, *J. Am. Chem. Soc.* 125 (2003) 2723.
- [32] J.M. Bonello, R. Lindsay, A.K. Santra and R.M. Lambert, *J. Phys. Chem. B* 106 (2002) 2672.
- [33] J.M. Bonello, R.M. Lambert, N. Künzle, A. Baiker, *J. Am. Chem. Soc.* 122 (2000) 9864.
- [34] M.A. Keane, *Langmuir* 13 (1997) 41.
- [35] M.A. Keane and G. Webb, *J. Catal.* 136 (1992) 1.
- [36] M.A. Keane and G. Webb, *J. Chem. Soc. Chem. Commun.* (1991) 1619.
- [37] A. Tai and T. Sugimura, in: *Chiral Catalyst Immobilization and Recycling*, (eds. D.E. De Vos, I.F.J. Vankekecom and P.A. Jacobs) (Wiley-VCH, Weinheim, 2000) p. 173.
- [38] T. Osawa, T. Harada and O. Takayasu, *Top. Catal.* 13 (2000) 155.
- [39] H.-J. Yan, D. Wang, M.-J. Han, L.-J. Wan and C.-L. Bai, *Langmuir* 20 (2004) 7360.
- [40] M.O. Lorenzo, S. Haq and T. Bertrams, P. Murray, R. Raval, C.J. Baddeley, *J. Phys. Chem. B* 103 (1999) 10 661.
- [41] M. Bowker, S. Haq, R. Holroyd, P.M. Parlett, S. Poulston and N. Richardson, *J. Chem. Soc. Faraday Trans.* 92 (1996) 4683.
- [42] F. Hahn, B. Beden and C. Lamy, *J. Electroanal. Chem.* 204 (1986) 315.
- [43] H.Q. Li, S.G. Roscoe and J. Lipkowski, *J. Electroanal. Chem.* 478 (1999) 67.
- [44] B.G. Frederick, Q. Chen, F.M. Leibsle, M.B. Lee, K.J. Kitching and N.V. Richardson, *Surf. Sci.* 394 (1997) 1.
- [45] S. Floate, M. Hosseini, M.R. Arshadi, D. Ritson, K.L. Young and R.J. Nichols, *J. Electroanal. Chem.* 542 (2003) 67.
- [46] R.J. Nichols, I. Burgess, K.L. Young, V. Zamylnny and J. Lipkowski, *J. Electroanal. Chem.* 563 (2004) 33.
- [47] D.P. Woodruff, C.F. McConville, A.L.D. Kilcoyne, Th. Linder, J. Somers, M. Somers, M. Surman, G. Paolucci and A.M. Bradshaw, *Surf. Sci.* 201 (1988) 228.

- [48] J. Somers, A.W. Robinson, Th. Linder and A.M. Bradshaw, *Phys. Rev. B.* 40 (1989) 2053.
- [49] J.R.B. Gomes and J.A.N.F. Gomes, *Surf. Sci.* 432 (1999) 279.
- [50] S. Bao, K.M. Schindler, P. Hofmann, V. Fritzsche, A.M. Bradshaw and D.P. Woodruff, *Surf. Sci.* 291 (1993) 295.
- [51] L.A.M.M. Barbosa and P. Sautet, *J. Am. Chem. Soc.* 123 (2001) 6639.
- [52] M.O. Lorenzo, V. Humblot, P. Murray, C.J. Baddeley, S. Haq and R. Raval, *J. Catal.* 205 (2002) 123.
- [53] T.E. Jones and C.J. Baddeley, *Surf. Sci.* 519 (2002) 237.
- [54] T.E. Jones and C.J. Baddeley, *Surf. Sci.* 513 (2002) 453.
- [55] B. Ohtani, A. Shintani and K. Uosaki, *J. Am. Chem. Soc.* 121 (1999) 6515.
- [56] T. Nakanishi, N. Yamakawa, T. Asahi, T. Osaka, B. Ohtani and K. Uosaki, *J. Am. Chem. Soc.* 124 (2002) 740.
- [57] X.-Y. Zhao, *J. Am. Chem. Soc.* 122 (2000) 12584.
- [58] G.A. Attard, A. Ahmadi, D.J. Jenkins, O.A. Hazzazi, P.B. Wells, K.G. Griffin, P. Johnston and J.E. Gillies, *Chem. Phys. Chem.* 4 (2003) 123.